Six Major Historical Earthquakes in the Seoul Metropolitan Area during the Joseon Dynasty (1392–1910)

Seongjun Park[1], Inho Baek[1], and Tae-Kyung Hong[*1]

ABSTRACT

Earthquake records in the historical literature provide valuable information on the seismic hazard potentials for long recurrence times. The Seoul metropolitan area is the center of the economy and infrastructure in South Korea. Six major earthquakes that occurred around the Seoul metropolitan area during the Joseon dynasty in 1392–1910 are analyzed using a probabilistic joint inversion method based on seismic damage records and earthquake-felt reports. The inversion yields sets of event locations and magnitudes with probabilities. The joint inversion method is validated with synthetic and instrumentally observed data sets. The historical earthquakes are found to be located around the Seoul metropolitan area. The magnitudes of the earthquakes range from M_L 5.3 to 6.8 at the peak probabilistic locations. These historical earthquakes suggest considerable seismic hazard potentials in the Seoul metropolitan area.

KEY POINTS

- Historical seismic-damage records of Korea are analyzed using a probabilistic inversion method.
- Six major earthquakes with magnitude 5.3–6.8 occurred around Seoul during the Joseon dynasty in 1392–1910.
- The historical earthquakes suggest considerable seismic hazard potentials in the Seoul metropolitan area.

Supplemental Material

INTRODUCTION

A series of major earthquakes occurred over time in the Korean Peninsula after the 2011 M_w 9.0 Tohoku-Oki megathrust earthquake (Hong *et al.*, 2018). There is increasing concern regarding the possible occurrence of major events in regions with large populations. A single major earthquake may cause fatal damage to large cities. Hence, it is crucial to assess the seismic hazard potentials around large cities.

The Seoul metropolitan area, which boasts a large population, is the center of the economy and infrastructure in South Korea. No major earthquakes have been observed in the Seoul metropolitan area according to instrumental records of seismicity (Houng and Hong, 2013; Hong *et al.*, 2016). However, the Korean Peninsula belongs to an intraplate regime where major earthquakes occur with long recurrence intervals (Shimazaki and Nakata, 1980; Schwartz and Coppersmith, 1984; Pearthree and Calvo, 1987). Thus, there is limitation to use short-term instrumental earthquake records for seismic hazard assessment. The seismic hazard potentials are assessed properly based on long-term records (Frankel, 1995; McGuire, 1995; Stirling *et al.*, 1998; Miyazawa and Mori, 2009). Historical seismicity can provide valuable information on the seismic hazard potentials for earthquakes with long recurrence intervals.

There are historical literatures that describe seismic damage and earthquakes during the Joseon dynasty in 1392–1910. The historical literatures include Joseon-Wangjo-Sillok (The Annals of the Joseon Dynasty), Seungjeongwon-Ilgi (Diaries of the Royal Secretariat), Ilseongnok (Records of Daily Reflections), and Bibyeonsa-Deungnok (Records of the Border Defense Council). However, records of historical earthquakes suffer from inherent uncertainties in the event locations and magnitudes.

There were rigorous attempts to determine the source parameters of historical earthquakes (Degasperi *et al.*, 1991; Wang, 2004; Lee and Yang, 2006; Korea Meteorological Administration, 2012). Previous studies estimated the source parameters deterministically, which may incorporate the errors associated with inherent uncertainty. These studies determined the event location to be the position with the most seismic

1. Department of Earth System Sciences, Yonsei University, Seoul, South Korea

*Corresponding author: tkhong@yonsei.ac.kr

Cite this article as Park, S., I. Baek, and T.-K. Hong (2020). Six Major Historical Earthquakes in the Seoul Metropolitan Area during the Joseon Dynasty (1392–1910), *Bull. Seismol. Soc. Am.* **110**, 3037–3049, doi: 10.1785/0120200004

damage or the area where the central earthquake was felt (Degasperi *et al.*, 1991; Wang, 2004; Lee and Yang, 2006). Isoseismal maps could also be used for the determination of event locations (Sibol *et al.*, 1987; Levret *et al.*, 1994; Albarello *et al.*, 1995; Termini *et al.*, 2005). In addition, the event magnitudes were determined from epicentral seismic intensities or the sizes of isoseismal areas.

A probabilistic inversion method for historical earthquakes was proposed to determine the earthquake magnitude and event location jointly (Houng and Hong, 2013). The method was modified to satisfy the Gutenberg–Richter frequency–magnitude relationship (Park and Hong, 2016). In this study, we apply the method for the source-parameter inversion of six major earthquakes around the Seoul metropolitan area during the Joseon dynasty.

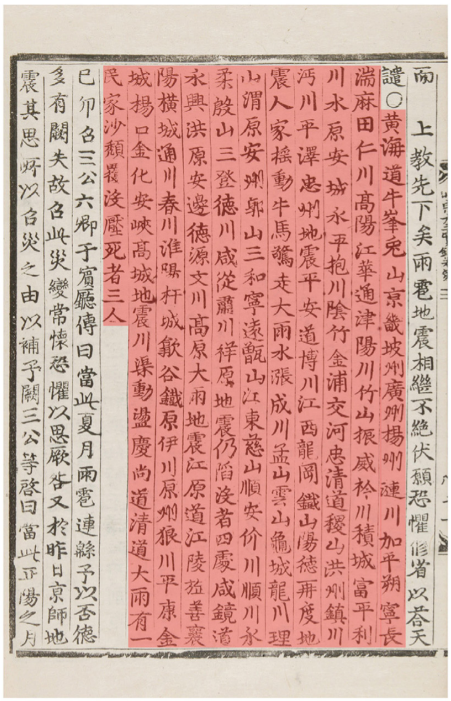

朝鮮王朝實錄
조선왕조실록 (Joseon-Wangjo-Sillok)
The Annals of the Joseon Dynasty

Seismic-damage record in June 20, 1546

黃海道牛峯兎山京畿坡州廣州楊州漣川加平朔寧長湍麻田仁川高陽江華通津陽川竹山振威衿川積城富平利川水原安城永平抱川陰竹金浦交河忠淸道稷山洪州鎭川沔川平澤忠州地震平安道博川江西龍岡鐵山陽德再度地震人家搖動牛馬驚走大雨水漲成川孟山雲山龜城龍川理山渭原安州郭山三和寧遠甑山江東慈山順安价川順川永柔殷山三登德川咸從肅川祥原地震仍陷沒者四處咸鏡道永興洪原安邊德源文川高原大雨地震江原道江陵旌善襄陽橫城通川春川淮陽杆城歙谷鐵原伊川原州狼川平康金城楊口金化安峽高城地震川渠動盪慶尙道淸道大雨有一民家沙頹覆沒壓死者三人

Figure 1. An example of historical seismic damage records for the 20 June 1546 earthquake in the Annals of the Joseon Dynasty (Joseon-Wangjo-Sillok). The part of seismic damage description is marked. Severe damages including house wall collapse happened in Seoul. Strong ground shaking were felt in most counties in the central and northern Korean Peninsula. The original document and contents are presented. The color version of this figure is available only in the electronic edition.

DATA AND SEISMOTECTONICS

Historical earthquake damage records for the Korean Peninsula were identified in various studies (Lee and Yang, 2006; Korea Meteorological Administration, 2012). We analyze the historical earthquake damage records in Joseon-Wangjo-Sillok and Seungjeongwon-Ilgi that are available from the National Institute of Korean History (Fig. 1). Joseon-Wangjo-Sillok is a government record compilation of daily events in 1392–1863 during Joseon dynasty. Seungjeongwon-Ilgi is a government diary that recorded the official business of the royal court in 1623–1894. Earthquake felt and damage records are available from the historical literatures. We additionally collect historical earthquake damages from historical literatures, including Jeungbo-Munheon-Bigo, Yongchundamjukgi, and Irakjeongjip (Korea Meteorological Administration, 2012).

We collect historical records of 1524 earthquakes in 1392–1910 (Lee and Yang, 2006; Korea Meteorological Administration, 2012). We choose historical earthquakes either with peak seismic intensities ≥7 on the modified Mercalli intensity (MMI) scale or with reports of the earthquake being felt in more than 10 cities or counties. We find 61 earthquakes that were felt in Seoul. We ultimately find that six major earthquakes occurred around the Seoul metropolitan area on 5 July 1503, 13 September 1503, 22 June 1518, 7 October 1531, 20 June 1546, and 16 July 1613. These earthquakes produced seismic damage over wide regions. These seismic damage estimates are converted into seismic intensities, while the earthquake-felt reports are translated into ranges of seismic intensities (see the supplemental material, available to this article).

The Korean Peninsula is located in an intraplate region along the far eastern margin of the Eurasian plate (Fig. 2). The eastern Eurasian plate collides with both the Philippine Sea plate and the Okhotsk plate. The plate collisions generate a stress field composed of east-northeast-directed compression and west-northwest-directed tension in the Korean Peninsula (H. Choi *et al.*, 2012; Lee *et al.*, 2017) (Fig. 2). The geological provinces of the Korean Peninsula are representative of three Precambrian massif blocks and two intervening belts (Chough *et al.*, 2000). The crustal thickness of the peninsula ranges within 29–36 km (Hong *et al.*, 2008; He and Hong, 2010).

The ambient stress field produces strike-slip earthquakes with strike orientations of predominantly northeast–southwest. Thrust earthquakes with strikes of north–south occur in the paleo-rift structure off the eastern coast of the peninsula. Normal-faulting earthquakes with strikes of east–west occur in the central Yellow Sea, where a continental collision belt may

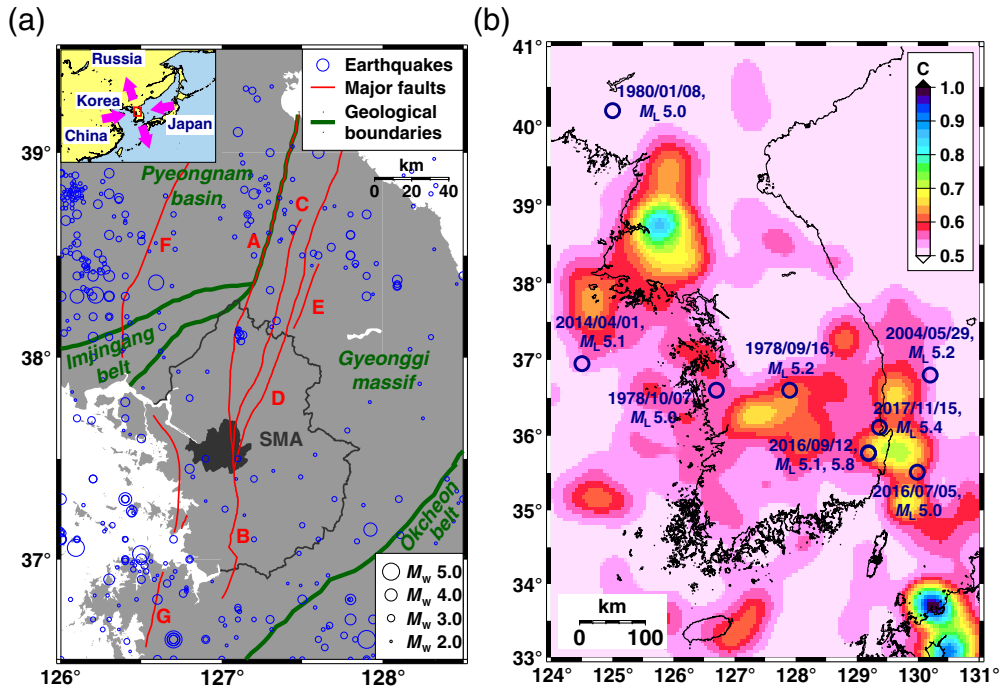

Figure 2. Seismicity and geological structures. (a) Major faults, geological provinces, and instrumental seismicity in the central Korean Peninsula. The faults include Chugaryeong fault (A), Singal fault (B), Pochen fault (C), Wangsukcheon fault (D), Jamgok fault (E), Yeseoggang fault (F), and Dangjin fault (G). The ambient stress field around the Korean Peninsula are presented with arrows (inset). (b) Seismicity densities and distribution of major earthquakes with magnitudes greater than or equal to M_L 5.0 around the Korean Peninsula since 1978. The instrumental earthquake records present low seismicity around the Seoul metropolitan area (SMA). The territory of Seoul is marked on the map. The color version of this figure is available only in the electronic edition.

exist (Hong and Choi, 2012). The Seoul metropolitan area is situated within a massif block (the Gyeonggi massif), where the frequency of seismicity is low with a long recurrence interval.

The Chugaryeong fault system is a major system of faults striking north-northeast and northeast across the Gyeonggi massif. The Chugaryeong fault system is composed of numerous Quaternary faults, including the Chugaryeong (Daeseongri), Pocheon, Wangsukcheon, and Singal faults, which are subparallel to one another (Kim, 1973; S.-J. Choi *et al.*, 2012; Chung *et al.*, 2014; Bae and Lee, 2016). The Chugaryeong fault system surrounds the Seoul metropolitan area, and earthquakes have been instrumentally recorded throughout the Chugaryeong fault system (Fig. 2).

We collect information of instrumentally recorded earthquakes that occurred around the Korean Peninsula during the period of 1978–2018 from the Korea Meteorological Administration (KMA), Japan Meteorological Agency (JMA), and China Earthquake Administration (CEA). The magnitudes from the KMA and CEA are converted to the moment magnitude scale using empirical relationships (Scordilis, 2006; Bormann *et al.*, 2007). The JMA magnitude scale (M_{JMA}) is nearly equivalent to the moment magnitude scale for shallow earthquakes (Katsumata, 1996; Oth *et al.*, 2010).

The moment magnitudes of major earthquakes are additionally collected from the Global Centroid Moment Tensor (Global CMT) catalog and previous studies (Hong and Choi, 2012; Hong *et al.*, 2017, 2018). The numbers of earthquakes from the KMA, JMA, and CEA earthquake catalogs with magnitudes greater than or equal to M_w 2.0 are 2861, 3484, and 147, respectively. The numbers of earthquakes with magnitudes greater than or equal to M_w 3.0 are 748, 647, and 147, respectively. The instrumental earthquake catalogs from these three institutes are combined, and duplicate records are removed. The dominant focal depths range between 4 and 16 km (Hong *et al.*, 2016). According to the instrumentally recorded seismicity, the maximum earthquake magnitude in the seismotectonic province that includes the Seoul metropolitan area is M 5.3–6.4 (Hong *et al.*, 2016).

METHOD

We apply a joint inversion method to determine the event locations and magnitudes of historical earthquakes. The posterior probability, R, of an event with a magnitude M at a location $\mathbf{x}$ is given by (Houng and Hong, 2013; Park and Hong, 2016)

$$R(\mathbf{x}, M) = L(\mathbf{x}, M) \times F(M) \times C(\mathbf{x}), \quad (1)$$

in which $L(\mathbf{x}, M)$ is the fitness function between the reference and observed seismic intensities, $F(M)$ is the relative occurrence frequency of earthquakes with the magnitude M, and $C(\mathbf{x})$ is the seismicity density at the location $\mathbf{x}$. The normalized posterior probability function, P, is given by

$$P(\mathbf{x}, M) = R(\mathbf{x}, M)/R_{\max}, \quad (2)$$

in which $R_{\max}$ is the largest R value.

The seismic-intensity fitness function $L(\mathbf{x}, M)$ is given by

$$L(\mathbf{x}, M) = \prod_{j=1}^{N} \int_{I_j^{\min}}^{I_j^{\max}} \exp\left[-\frac{\{q - I_j^{\text{ref}}(\mathbf{x}, M)\}^2}{2\sigma^2}\right] dq, \quad (3)$$

in which N is the number of sites with reports in which the earthquake was felt, $I_j^{\max}$ is the upper bound of the seismic intensity at site j, $I_j^{\min}$ is the lower bound of the seismic intensity at site j, $I_j^{\text{ref}}(\mathbf{x}, M)$ is the theoretical seismic intensity expected at site j when an event of magnitude M occurs at a location $\mathbf{x}$, and σ is a constant accounting for possible differences between the observed and theoretical seismic intensities. We set σ to be 0.65 in MMI unit (Park and Hong, 2017).

The reference seismic intensity at site j, I_j^{ref}, is given by (Park and Hong, 2017)

$$I_j^{\text{ref}}(\mathbf{x}, M) = c + \alpha M - \beta \ln d - \gamma d, \tag{4}$$

in which M is the event magnitude, $\mathbf{x}$ is the event location, d is the hypocentral distance from the event, and c, α, β, and γ are site-dependent constants. We assume the focal depth to be 10 km. The constants c, α, β, and γ are set to −0.998, 1.72, 0.644, and 0.00608, respectively (Park and Hong, 2017). The relative earthquake occurrence frequency, $F(m)$, is given by

$$F(m) = 10^{-bm}, \tag{5}$$

in which b is the constant of the Gutenberg–Richter frequency–magnitude relationship and is set to 0.92 (Park and Hong, 2016). We set the seismicity density function $C(\mathbf{x})$ to vary between 0.5 and 1.0.

The seismic-intensity fitness function is dependent on the accuracy and uncertainty in seismic-intensity data points. Loosely constrained seismic-intensity values are applicable to the inversion.

ANALYSIS

The instrumentally observed earthquakes with magnitudes larger than or equal to M_w 3.0 are declustered using a nonparametric method (Marsan and Lenglinè, 2008; Hong *et al.*, 2018). We smooth the seismicity densities of the declustered instrumentally recorded seismicity with magnitudes $M_w \geq 3.0$ using a Gaussian function with a correlation distance of 20 km (Kossobokov *et al.*, 2000; Houng and Hong, 2013; Hong *et al.*, 2016). We then construct the seismicity density function by normalizing the smoothed seismicity densities to which uniform seismicity densities are added.

We assign a seismic-intensity value to each description of seismic damages and animal responses considering the common definitions of MMI scales (Wood and Neumann, 1931; Richter, 1958). The assignment of seismic intensities needs consideration on the properties of urban environments, building structures, and construction materials (Ambraseys and Douglas, 2004; Musson *et al.*, 2010; Astroza *et al.*, 2012; Bakun *et al.*, 2012; Musson and Cecić, 2012). The houses in the Korean Peninsula during the Joseon dynasty may belong to the categories of masonry C or D (Richter, 1958; Ministry of Construction and Transportation, 1997). We introduce the seismic-intensity assignment criteria for the seismic damages considering the vulnerability of historical building structures (Ministry of Construction and Transportation, 1997; Korea Meteorological Administration, 2012) (Table 1). We assign seismic-intensity ranges instead of single seismic-intensity values to reflect possible differences in description for common seismic damages (Grünthal, 1998; Musson, 1998).

TABLE 1
Seismic Damage Description and Corresponding Seismic Intensity

Description	Seismic Intensity (MMI)
Birds flying and crying	4–6
House shaking	5–6
Shaking roofing tile	5–6
Domestic animals running away	5–6
Streams rippling	5–7
Roof tile falling	6–7
House wall and fence collapsing	7–8
Rocks rolling down a mountainside	7–8
Castle battlement collapsing	7–8
Water spilling out from a dried creek	8–9
Seawater swaying and bubbling	8–9
Houses collapsing	8–9
Felt reports without damage description	3–8

MMI, modified Mercalli intensity.

Some earthquake records lack a specific description of seismic damage, presenting only the information that the earthquakes were felt by people in indicated regions. We consider a range of seismic intensities for these reports considering the seismic-intensity distribution for earthquakes in the Korean Peninsula (Park and Hong, 2017). Ground motions associated with MMI 2 or less are rarely felt by the public. Also, seismic damage associated with MMI 9 or higher is rare on the Korean Peninsula. We assign seismic intensities of MMI 3–8 to the felt reports. However, when the peak seismic damage corresponds to a seismic intensity of MMI 9, we set the possible seismic-intensity range to be MMI 3–9.

It is difficult to infer the focal depths of earthquakes from historical records of seismic damage. We assume a reference focal depth of 10 km, considering the typical focal depths (4–16 km) of instrumentally recorded earthquakes in the Korean Peninsula (Hong *et al.*, 2016). The calculated magnitudes are hardly affected by an assumed focal depth, when the seismic intensities at epicentral distances greater than 10 km are implemented in the analysis ($\Delta M < 0.1$).

We next determine the location and magnitude of each event that satisfy the observed attenuation of the seismic intensity with distance. We find the optimum set an event location and magnitude by minimizing the misfit errors between the reference seismic-intensity curves and observed seismic intensities.

VALIDATION TESTS

This study performs a joint inversion method to determine the source location and magnitude simultaneously based on

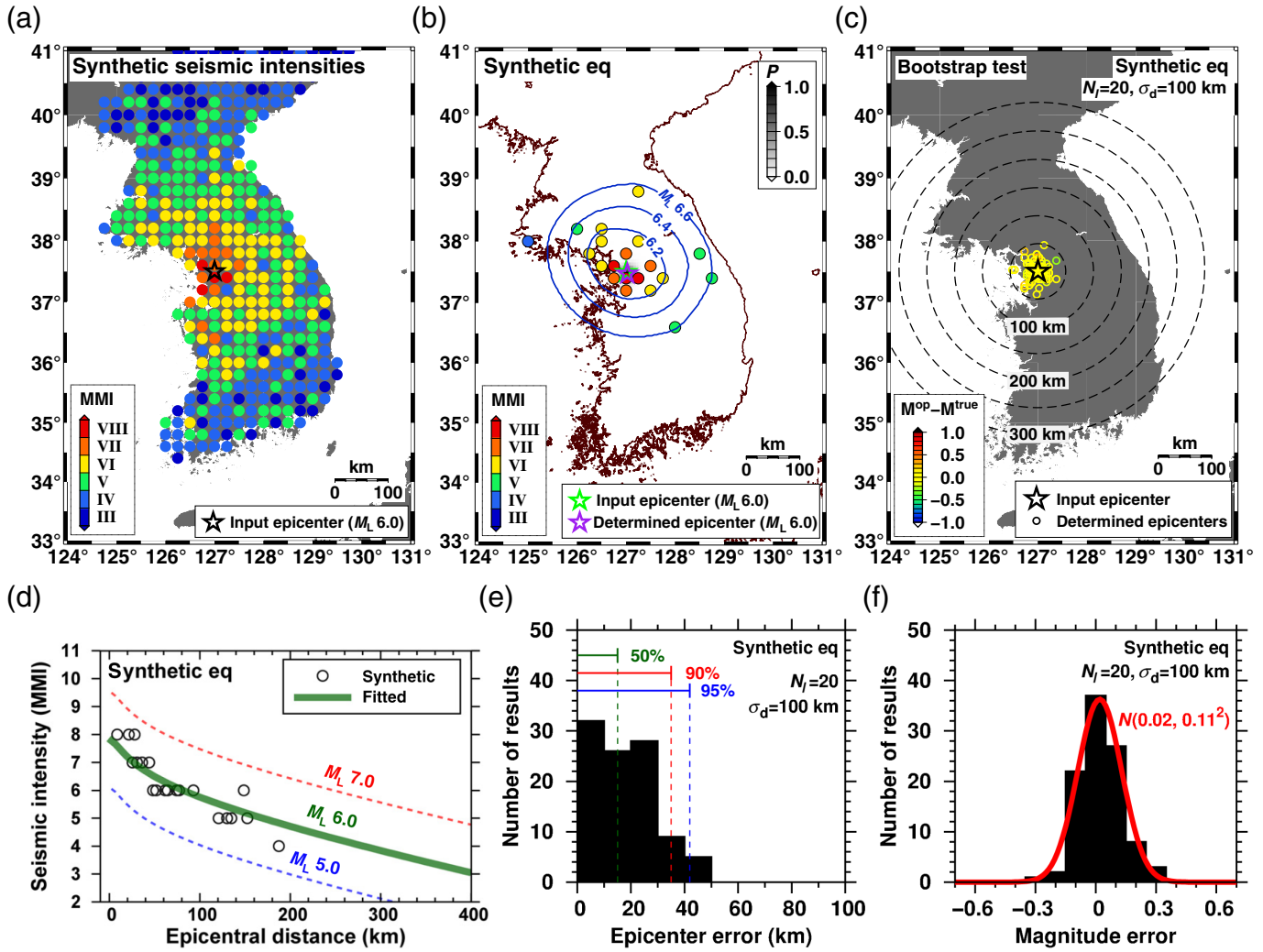

limited available records. We produce synthetic seismic-intensity data for a fictitious earthquake in the Seoul metropolitan area. We consider an earthquake with a magnitude of M_L 6.0 and a focal depth of 10 km. We add random errors to the synthetic seismic intensities with a standard deviation of 0.65 in MMI unit considering the level of seismic-intensity anomalies in the Korean Peninsula (Park and Hong, 2017) (Fig. 3). We collect the seismic intensities at 20 randomly selected locations. The weight at a randomly selected location is inversely proportional to the distance. In this way, we compose 100 sets of synthetic seismic-intensity data.

We find that the event locations are placed within a distance of 40 km from the considered location in 95% of the inversion results (Fig. 3). The inverted event magnitudes present an average difference of 0.02 in MMI unit from the considered event magnitude, and the standard deviation is 0.11 in MMI unit. These observations show that the event locations and magnitudes are reasonably determined (Fig. 3).

We further test the method with field data for an instrumentally recorded earthquake with known source parameters (Fig. 4). We consider the 12 September 2016 M_L 5.8 earthquake, the largest event to strike the Korean Peninsula since 1952. This earthquake occurred along a fault plane at depths of 11–16 km (Hong *et al.*, 2017). The strike of the fault is N27°E, and the dip is 65°. The observed peak ground accelerations reached 4.4 m/s^2 on the horizonal components and 2.3 m/s^2 on the vertical component. The peak seismic intensity was MMI 8 around the epicenter (Hong *et al.*, 2017).

Figure 3. Validation test with synthetic data sets. (a) Distribution of the synthetic seismic intensity for an event with a magnitude of M_L 6.0 and a focal depth of 10 km. The event location and magnitude are indicated. (b) An example of an inversion based on a synthetic data set composed of 20 randomly selected seismic intensities. The distribution of seismic intensities and probabilities is presented. (c) Locations of the peak probabilities for 100 synthetic data sets. The magnitude errors are presented. (d) An example of fitting with a seismic-intensity attenuation curve for an event at the peak probability location. (e) Location errors with respect to the input locations. Approximately 95% of the inversions yield location errors smaller than 40 km. (f) Magnitude errors with respect to the input magnitudes. The average magnitude error is 0.02 in modified Mercalli intensity (MMI) unit, and the standard deviation is 0.11 in MMI unit. The color version of this figure is available only in the electronic edition.

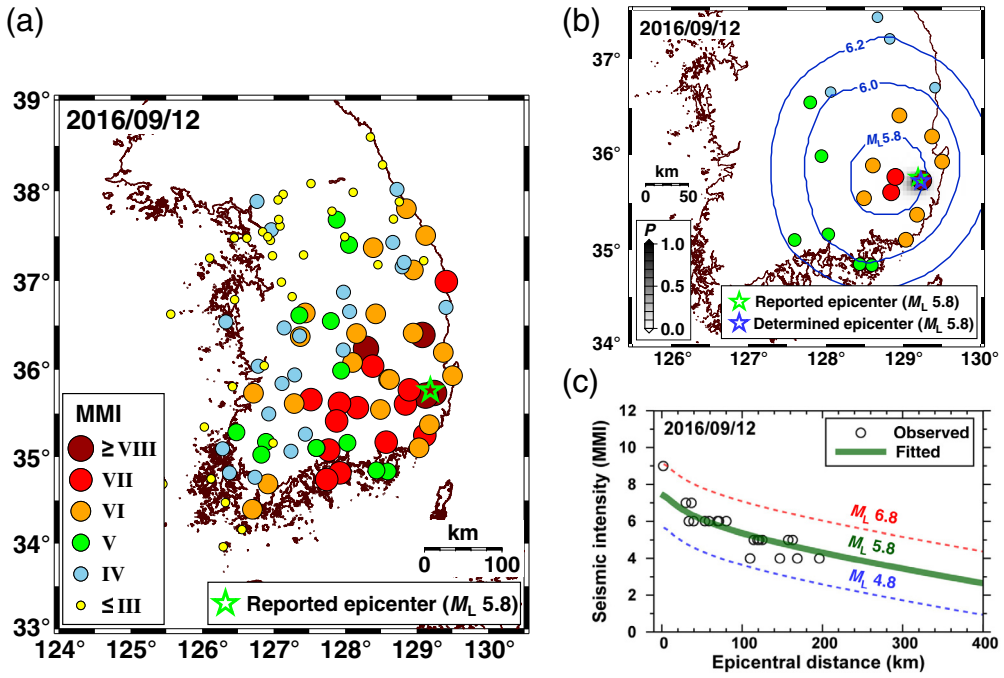

Figure 4. Inversion based on instrumentally recorded seismic-intensity data for the 12 September 2016 M_L 5.8 Gyeongju earthquake. (a) Spatial distribution of the seismic intensities. (b) Inversion based on 20 randomly selected seismic intensities. The event magnitude and location are well determined. (c) Seismic intensities and inverted seismic-intensity attenuation curve for an M_L 5.8 event at the peak probability location. The seismic-intensity attenuation curve represents the observed seismic intensities reasonably. The color version of this figure is available only in the electronic edition.

The earthquake was located close to the coast. Thus, the spatial distribution of earthquake-felt regions was uneven from the epicenter. The earthquake was well recorded at 160 seismic stations throughout the Korean Peninsula. We determine the event location and magnitude based on the seismic intensities at 20 randomly selected locations. The inverted event location and magnitude match reasonably well with the reported source parameters (Fig. 4). These inversion results indicate that this method can determine the source location and magnitude from the seismic intensity of the event.

INVERSION WITH LOOSELY CONSTRAINED SEISMIC INTENSITIES

Seismic intensities can be loosely constrained for historical earthquake records with unspecified seismic-damage description, animal reaction, and natural phenomena. We assign seismic-intensity ranges for such historical records. We test the stability and accuracy of source-parameter inversion for the implementation of seismic-intensity range data in which seismic-intensity uncertainty is naturally incorporated.

We consider a fictitious earthquake with magnitude M_L 6.0 in the Seoul metropolitan area. We assign seismic-intensity ranges at 20 randomly selected sites (Fig. 5). We set the lower bound of seismic intensities to be MMI 3, considering the typical lowest seismic intensity in regions where most people feel the seismic ground motions. We produce 100 sets of synthetic seismic-intensity data.

First, we consider an ideal situation in which the medians of seismic-intensity ranges are aligned with the theoretical ground-motion levels (Fig. 5b). We consider the seismic-intensity uncertainty of 2 in MMI unit (i.e., ±1 in MMI unit from the theoretical curve). We find that 99% of inversions yield the location and magnitude errors less than 20 km and 0.1 magnitude unit.

We further consider a situation with a larger seismic-intensity uncertainty of 4 in MMI unit (±2 in MMI unit) (Fig. 5c). We find that 95% inversions based on the data sets yield location and magnitude errors less than 21 km and 0.1 magnitude unit.

We now consider a case of seismic-intensity ranges with perturbations. This case represents a situation with inconsistent assignment of seismic-intensity ranges, which often happens in practical application. We produce seismic-intensity range datasets with uncertainty of 4 in MMI unit with additional random perturbations of −2 to 2 in MMI unit (Fig. 5d). We find that 90% of inversions yield location and magnitude errors of less than 45 km and 0.2 in magnitude unit.

We finally examine the inversion performance for a situation with a fewer number of seismic-intensity range data points. We consider seismic-intensity ranges at 10 randomly selected locations. We find that 90% of inversions yield the location and magnitude errors less than 54 km and 0.3 magnitude unit (Fig. 5). These tests suggest that the event locations and magnitudes can be determined reasonably with datasets composed of loosely constrained seismic-intensity ranges.

HISTORICAL EARTHQUAKES

We determine the source parameters of the six major earthquakes that occurred around the Seoul metropolitan area during the Joseon dynasty. We present the spatial distributions of the probabilities of the event locations and associated magnitudes. The event locations and magnitudes are compared with those determined in a previous study (Lee and Yang, 2006). The complete lists of assigned seismic intensities for earthquakes are presented in the supplemental material (Tables S1–S6).

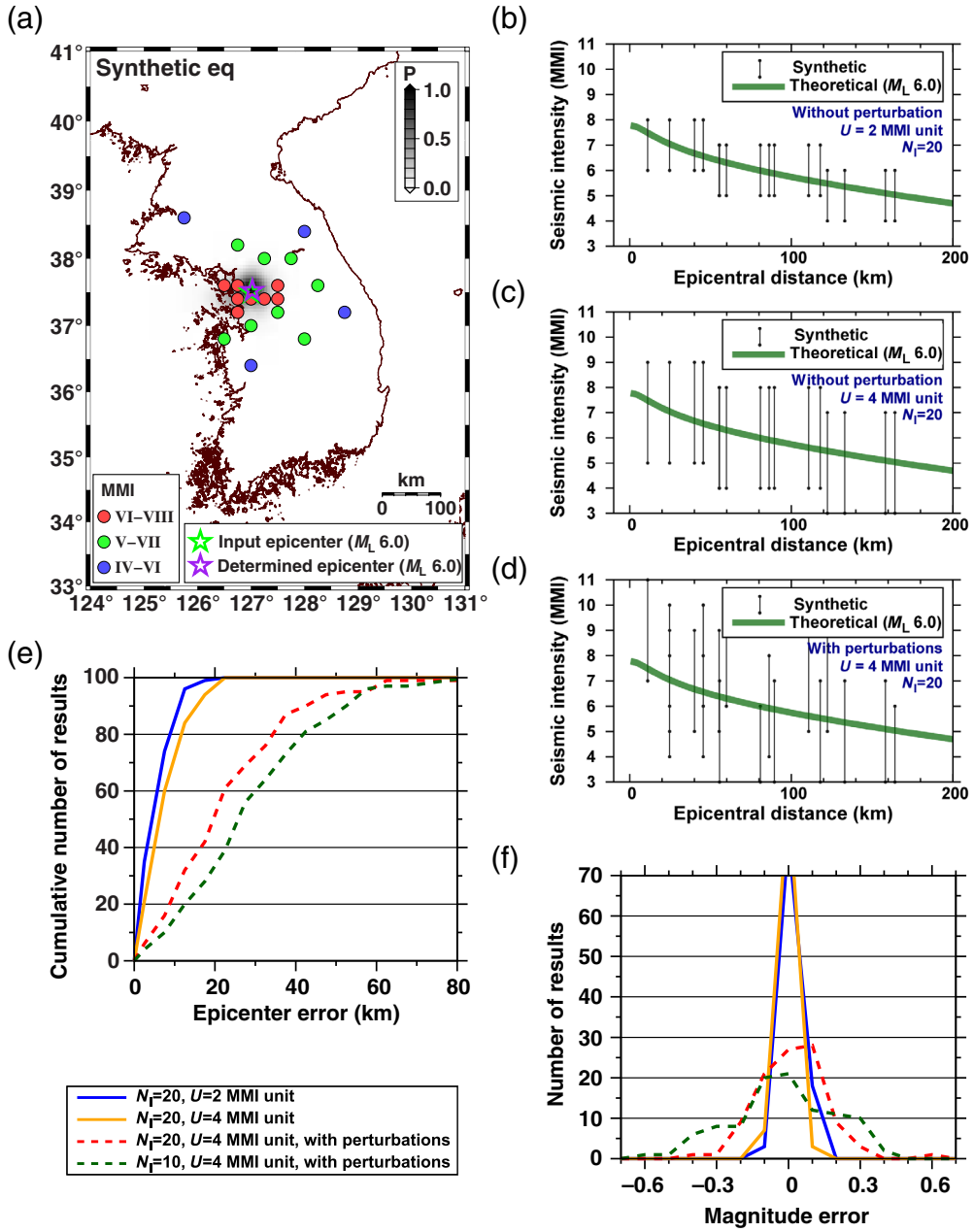

Figure 5. Source-parameter inversions with seismic-intensity ranges for a fictitious earthquake with magnitude M_L 6.0. (a) An example of inversion. The event location and synthetic seismic intensities at randomly selected locations are presented. The location of peak probability is indicated. Input seismic-intensity ranges with uncertainties U of (b) 2 in MMI unit (±1 in MMI unit) and (c) 4 in MMI unit (±2 in MMI unit) along the theoretical seismic-intensity attenuation curve, and (d) with random perturbations of 4 in MMI unit (±2 in MMI unit). Error distribution in (e) epicenters and (f) magnitudes from the source-parameter inversions in different conditions. The source-parameter inversions yield reasonable results for all cases. The color version of this figure is available only in the electronic edition.

The 5 July 1503 event

The regions in which the earthquake was felt are indicated clearly. The earthquake was felt in 33 counties in the west-central peninsula, including Seoul. The earthquake was felt in an area over a radius of ~110 km (Fig. 6). These regions are laid over three prefectures (Gyeonggi-do, Chungcheongnam-do, and Chungcheongbuk-do). The seismic intensity for the regions with felt reports ranges from MMI 3 to 8. The highest probability is found at 36.875° N, 127.125° E, which approximately corresponds to the center of the earthquake-felt regions. The spatial distribution of earthquake-felt regions appears circular, which reduces the likelihood that the event occurred in an offshore region of the Yellow Sea. The magnitude is M_L 5.3 for focal depths of 4–16 km at the location with the peak probability. The event magnitude may vary between M_L 5.3 and 5.6 for locations with probabilities greater than 0.7.

The 13 September 1503 event

This earthquake occurred two months after the 5 July 1503 event. The earthquake was felt in 74 counties throughout the west-central peninsula from the west coast to the center of the peninsula. The radius of regions in which the earthquake was felt is ~120 km, which is larger than the corresponding radius of the 5 July 1503 event (Fig. 7). The felt regions encompass those, including Seoul, of the 5 July 1503 event (Figs. 6 and 7). The felt regions are distributed over four prefectures (Gyeonggi-do, Chungcheongnam-do, Chungcheongbuk-do, and Gyeongsangbuk-do). The earthquake-felt regions are situated closely around the intersection among Gyeonggi-do, Chungcheongnam-do, and Chungcheongbuk-do, and the number of these regions decreases with increasing distance from Seoul.

We assign the seismic intensities in the earthquake-felt regions to range from MMI 3 to 8. We find the location of

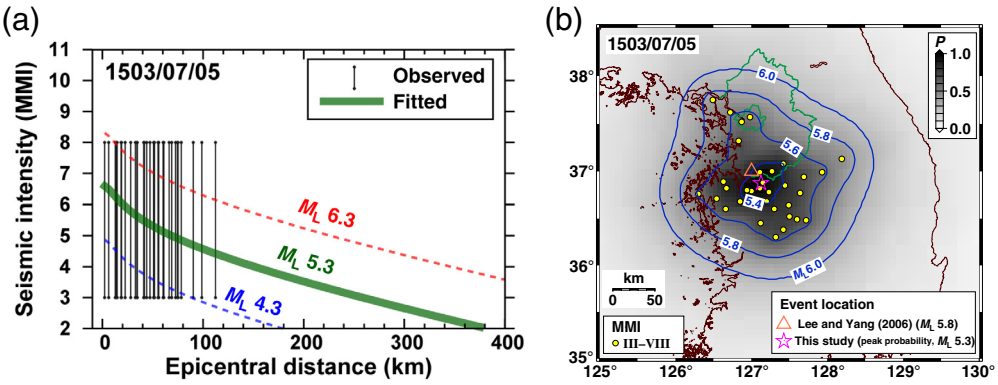

Figure 6. Determination of the magnitude and location of the 5 July 1503 earthquake. (a) Distribution of the seismic intensities and seismic-intensity attenuation curve for the magnitude and location set with the highest probability. The seismic-intensity attenuation curves for ±1 magnitude differences are presented for comparison. (b) Map of the seismic intensities and probability distribution. The location of the highest probability is marked (star). The event magnitudes at different locations are marked in contours. The territories of Seoul and Seoul metropolitan area are marked on the map. The color version of this figure is available only in the electronic edition.

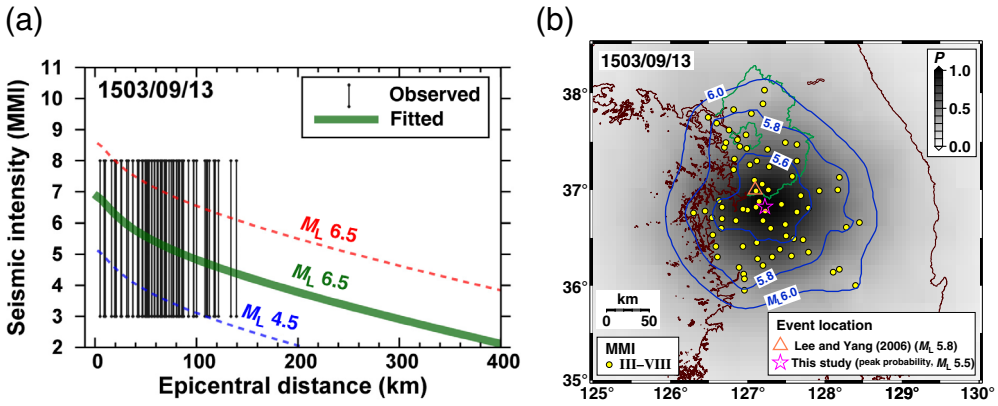

Figure 7. Determination of the magnitude and location of the 13 September 1503 earthquake. (a) Distribution of the seismic intensities and seismic-intensity attenuation curve for the magnitude and location set with the highest probability. The seismic-intensity attenuation curves for ±1 magnitude differences are presented for comparison. (b) Map of the seismic intensities and probability distribution. The location of the highest probability is marked (star). The event magnitudes at different locations are marked in contours. The territories of Seoul and Seoul metropolitan area are marked on the map. The color version of this figure is available only in the electronic edition.

the peak probability to be 36.825° N, 127.225° E. The magnitude at this location is M_L 5.5 for focal depths of 4–16 km, and the magnitudes at locations with probabilities greater than 0.7 are M_L 5.5–5.7.

The 22 June 1518 event

The seismic damage of this event was described for two regions, including Seoul and a suburb of the city. This earthquake, which was felt nationwide, induced the collapse of castles and houses in Seoul. The royal palace was shaken considerably. Many people lost consciousness, and people and horses were knocked off their feet by the shaking of the ground. People stayed outside their homes to avoid being inside a collapsing house.

A series of three to four earthquakes with strong ground motions occurred during the day of the event. Earthquakes continued throughout the night. The aftershocks continued for a month, and the earthquake occurrence frequency decreased with time. At least one earthquake struck each day of the month. The seismic damage to the Seoul metropolitan area induced by this event may be the most devastating among all six historical earthquakes. The reported seismic damage can be a consequence of a series of earthquakes in the region. In this study, we assume that the major seismic damage was caused by the mainshock.

We choose eight prefectures as reference locations for the felt reports. We assign the seismic intensity in Seoul to range from MMI 8 to 9. The seismic intensities for the felt regions are set to range from MMI 3 to 9. The location of the peak probability is found at 37.375° N, 127.025° E (Fig. 8). The magnitude at the location of the peak probability may be M_L 6.8 for focal depths of 4–16 km, and the magnitudes at locations with probabilities greater than 0.7 are M_L 6.7–7.1.

The 7 October 1531 event

This earthquake produced strong ground motions in Seoul. The earthquake was reportedly accompanied by loud sounds resembling thunder. The earthquake was felt in 28 counties throughout the central peninsula from the west coast to the east coast. The earthquake-felt regions are distributed over five prefectures in the center of the peninsula (Gyeonggi-do, Chungcheongbuk-do, Gyeongsangbuk-do, Gangwon-do, and Hwanghae-do). We observe a large number of regions in Gangwon-do and Hwanghae-do to the north and east of Seoul.

The seismic damage in Seoul corresponds to seismic intensities of MMI 5–6. The seismic intensities for the regions with

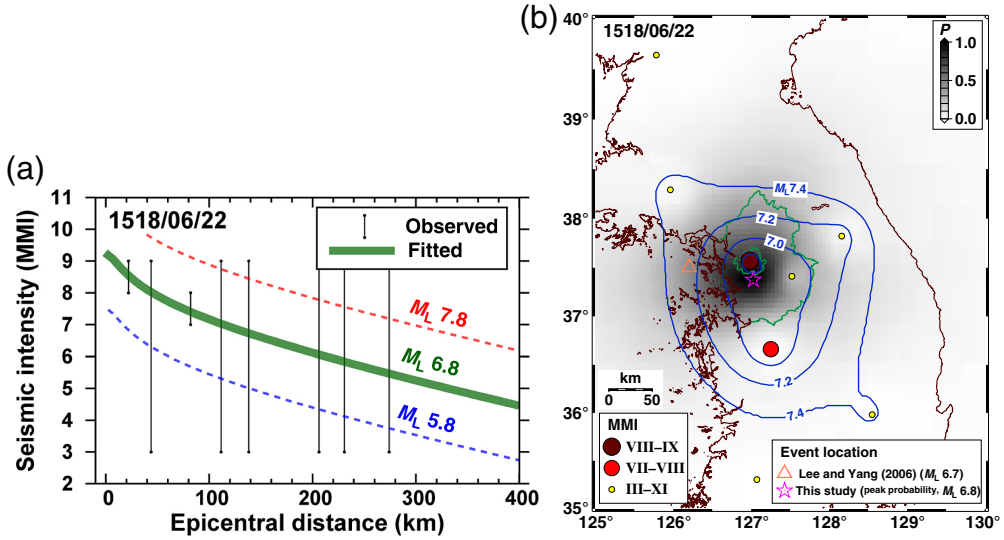

Figure 8. Determination of the magnitude and location of the 22 June 1518 earthquake. (a) Distribution of the seismic intensities and seismic-intensity attenuation curve for the magnitude and location set with the highest probability. The seismic-intensity attenuation curves for ±1 magnitude differences are presented for comparison. (b) Map of the seismic intensities and probability distribution. The location of the highest probability is marked (star). The event magnitudes at different locations are marked in contours. The territories of Seoul and Seoul metropolitan area are marked on the map. The color version of this figure is available only in the electronic edition.

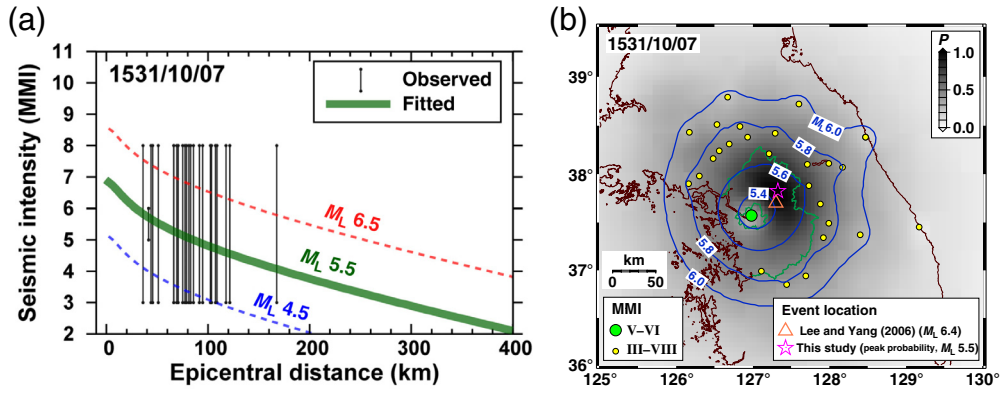

Figure 9. Determination of the magnitude and location of the 7 October 1531 earthquake. (a) Distribution of the seismic intensities and seismic-intensity attenuation curve for the magnitude and location set with the highest probability. The seismic-intensity attenuation curves for ±1 magnitude differences are presented for comparison. (b) Map of the seismic intensities and probability distribution. The location of the highest probability is marked (star). The event magnitudes at different locations are marked in contours. The territories of Seoul and Seoul metropolitan area are marked on the map. The color version of this figure is available only in the electronic edition.

felt reports are set to range from MMI 3 to 8. The location of the peak probability is placed at 37.825° N, 127.325° E (Fig. 9). The magnitude at the location of the peak probability may be M_L 5.5 for focal depths of 4–16 km, and the event magnitudes at locations with probabilities greater than 0.7 are M_L 5.3–5.7.

The 20 June 1546 event

This earthquake was felt in 89 counties over eight prefectures (Gyeonggi-do, Chungcheongnam-do, Chungcheongbuk-do, Gangwon-do, Hwanghae-do, Pyeonganbuk-do, Pyeongannam-do, and Hamgyeongnam-do) in the central and northern Korean Peninsula. Aftershocks continued throughout the day. The sound of thunder was heard during the main event, and houses and walls in Seoul collapsed. Domestic animals ran away as a result of the earthquake. Counties in Gangwon-do reported swelling in streams and rivers. In Pyeongan-do, cows and horses were frightened and ran away. Some counties reported flooding during the earthquake. The earthquake produced strong ground shaking that propagated from east to west in Seoul, which may suggest wave propagation or successive aftershocks.

We assign a seismic-intensity range of MMI 7–8 for Seoul. We set the seismic-intensity ranges for the earthquake-felt regions outside Seoul to be MMI 5–7, 4–6, or 3–8 depending on the locations and earthquake damage descriptions. The seismic-intensity range of MMI 5–7 is applied for the regions with swelling in streams and rivers (see supplemental material) (Grünthal, 1998; Korea Meteorological Administration, 2012). We assign seismic-intensity ranges of MMI 4–6 to the regions with animal reaction to the earthquake. Also, we assign MMI 3–8 to the earthquake-felt locations without particular description to cover all possible ranges of seismic damage.

The inversion searches all possible sets of source parameters for the loosely constrained seismic-intensity data sets. We find the most probable set of source parameter from the posterior probabilities. The location of the peak probability is placed at 37.675° N, 127.225° E (Fig. 10). The magnitude at the location of the highest probability may be M_L 6.2 for focal depths of 4–16 km, and the event magnitudes at

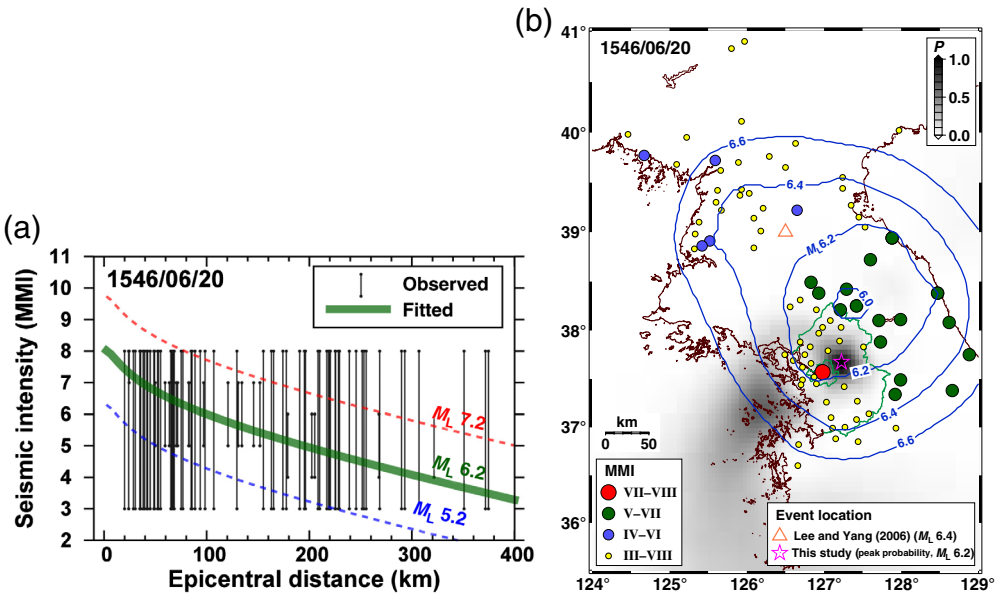

Figure 10. Determination of the magnitude and location of the 20 June 1546 earthquake. (a) Distribution of the seismic intensities and seismic-intensity attenuation curve for the magnitude and location set with the highest probability. The seismic-intensity attenuation curves for ±1 magnitude differences are presented for comparison. (b) Map of the seismic intensities and probability distribution. The location of the highest probability is marked (star). The event magnitudes at different locations are marked in contours. The territories of Seoul and Seoul metropolitan area are marked on the map. The color version of this figure is available only in the electronic edition.

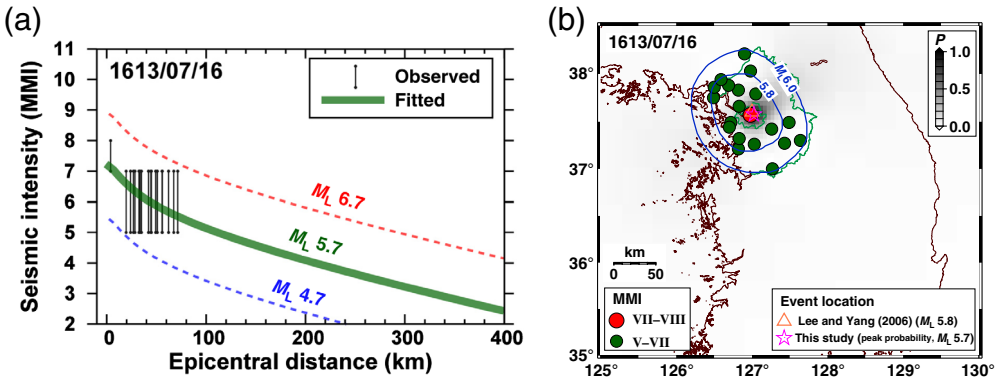

Figure 11. Determination of the magnitude and location of the 16 July 1613 earthquake. (a) Distribution of the seismic intensities and seismic-intensity attenuation curve for the magnitude and location set with the highest probability. The seismic-intensity attenuation curves for ±1 magnitude differences are presented for comparison. (b) Map of the seismic intensity and probability distribution. The location of the highest probability is marked (star). The event magnitudes at different locations are marked in contours. The territories of Seoul and Seoul metropolitan area are marked on the map. The color version of this figure is available only in the electronic edition.

locations with probabilities greater than 0.7 vary between M_L 6.1 and 6.2.

The 16 July 1613 event

Seismic damage was reported for regions in the west-central peninsula, including Seoul. The earthquake occurred at night (between 1 and 3 a.m.). The event was accompanied by a loud sound that was heard by many people. The ground shaking amplitude was large, and many house fences fell down in Seoul. The earthquake was felt over one prefecture (Gyeonggi-do). The earthquake propagated from northwest to southeast with the sound of thunder in a suburb region. The tiles on rooftops trembled.

We assign the seismic intensity in Seoul to be MMI 7–8. We choose the major location to be in Gyeonggi-do, and the seismic intensity is set to MMI 5–7. The highest probability location is determined to be 37.575° N, 127.025° E (Fig. 11). The magnitude at the location of the highest probability may be 5.7 for focal depths of 4–16 km, and the magnitude may vary by location. The event magnitudes at locations with probabilities greater than 0.7 are M_L 5.6–5.7.

DISCUSSION AND CONCLUSIONS

Seoul is the capital city of South Korea. The population is high. Recent increases in seismicity throughout the Korean Peninsula have raised concerns about seismic hazard potentials. Historical records of earthquakes are useful for assessing the seismic hazard potentials of events with long recurrence times. Hence, the historical literature provides valuable information on historical earthquakes. However, the historical records have inherent limitations with regard to the completeness of their records. Accounts of seismic damage and earthquake-felt regions may be listed selectively by the authors. Thus, historical earthquakes may suffer from inherent uncertainties in the inferred source parameters. The determination of single locations and magnitudes may exclude other possibilities.

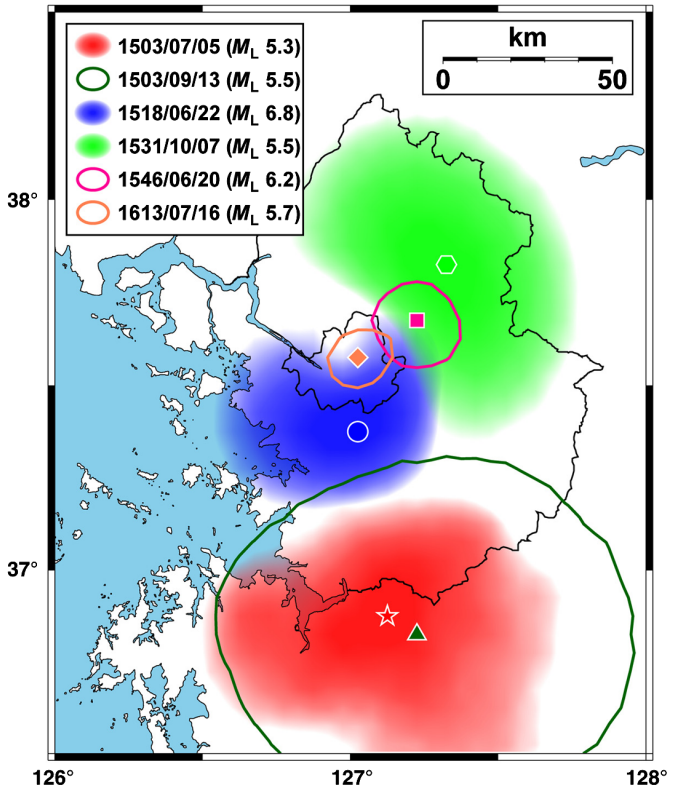

Figure 12. Possible source regions of the six major earthquakes that occurred around the Seoul metropolitan area. The areas of probabilities greater than 0.7 are presented. The locations of the peak probabilities are marked. The color version of this figure is available only in the electronic edition.

We introduced a probabilistic joint inversion method to determine the magnitudes and locations of events based on seismic intensities inferred from the seismic damage described in the historical literature. This approach allows us to consider possible sets of locations and magnitudes and presents the probability of each location and magnitude set. We assessed the errors caused by the uncertainty in seismicity intensity datasets. We found that the source parameters of historical earthquakes could be determined reasonably, despite possible inclusion of seismicity-intensity uncertainty. The optimal locations and magnitudes of earthquakes may be constrained with the help of other information, including geological features and instrumentally recorded seismicity.

We examined six major earthquakes that occurred around the Seoul metropolitan area during the Joseon dynasty. The probability distributions of the locations of the 20 June 1546 and 16 July 1613 events were well constrained compared with those of the other events (Fig. 12). The 22 June 1518 event and the 16 July 1613 event appeared to occur in the central Seoul metropolitan area; in particular, the 16 July 1613 event appeared to occur in Seoul. On the other hand, it appears that the 7 October 1531 event and the 20 June 1546 event occurred in the northeastern part of the Seoul metropolitan area. The 5 July 1503 event and the 13 September 1503 event appeared to occur in the southern Seoul metropolitan area; these two events have a time interval of ~2 months, which suggests that their occurrences are linked.

It is intriguing to note that the six major earthquakes were temporally clustered in 1546–1613. The seismicity appeared to be high in the sixteenth to seventeenth centuries (Lee and Yang, 2006; Houng and Hong, 2013). The major-earthquake surge may be related with the nature of seismicity in stable intraplate environment (Crone *et al.*, 2003; Holbrook *et al.*, 2006; Stein and Mazzotti, 2007; Li *et al.*, 2009). The temporal clustering of seismicity may be useful to understand the time-dependent recurrence characteristics of major earthquakes in stable intraplate regime.

The epicenters of six earthquakes were found to be located around the Seoul metropolitan area. The magnitudes of the events at the locations of their peak probabilities ranged between M_L 5.3 and 6.8. According to the analysis results, it is highly probable that moderate- or large-magnitude earthquakes occurred during the Joseon dynasty. This analysis suggests high seismic hazard risks in the Seoul metropolitan area. It may be possible to resolve the faults responsible for these earthquakes upon acquiring additional information.

DATA AND RESOURCES

The full description of seismic damages of historical earthquakes during the Joseon dynasty is available in Joseon-Wangjo-Sillok and Seungjeongwon-Ilgi (http://history.go.kr/). The instrumental earthquake catalogs are available from the Korea Meteorological Administration (http://necis.kma.go.kr/), Japan Meteorological Agency (https://www.data.jma.go.jp/), and International Seismological Centre (http://www.isc.ac.uk/iscbulletin/). All websites were last accessed in May 2020. The historical seismic-damage description in Joseon-Wangjo-Sillok and assigned seismic intensities for the six analyzed earthquakes are presented in the supplemental material.

ACKNOWLEDGMENTS

The authors thank Associate Editor Richard Briggs, Editor-in-Chief Thomas Pratt, and two anonymous reviewers for fruitful review comments. This work was supported by the Korea Meteorological Administration Research and Development Program under Grant Number KMI2018-02910. Additionally, this research was partly supported by the Basic Science Research Program of National Research Foundation of Korea (NRF-2017R1A6A1A07015374, NRF-2018R1D1A1A09083446).

REFERENCES

Albarello, D., A. Berardi, C. Margottini, and M. Mucciarelli (1995). Macroseismic estimates of magnitude in Italy, *Pure Appl. Geophys.* **145,** 297–312.

Ambraseys, N. N., and J. Douglas (2004). Magnitude calibration of north Indian earthquakes, *Geophys. J. Int.* **159,** 165–206.

Astroza, M., S. Ruiz, and R. Astroza (2012). Damage assessment and seismic intensity analysis of the 2010 (M_w 8.8) Maule earthquake, *Earthq. Spectra* **28,** no. S1, S145–S164.

Bae, H.-K., and H.-K. Lee (2016). Quaternary activity patterns of the Wangsukcheon Fault in the Pocheon-Namyangju area, Korea, *J. Geol. Soc. Korea* **52,** no. 2, 129–147 (in Korean with English abstract).

Bakun, W. H., C. H. Flores, and U. S. ten Brink (2012). Significant earthquakes on the Enriquillo fault system, Hispaniola, 1500-2010: Implications for seismic hazard, *Bull. Seismol. Soc. Am.* **102,** no. 1, 18–30.

Bormann, P., R. Liu, X. Ren, R. Gutdeutsch, D. Kaiser, and S. Castellaro (2007). Chinese national network magnitudes, their relation to NEIC magnitudes, and recommendations for new IASPEI magnitude standards, *Bull. Seismol. Soc. Am.* **97,** 114–127.

Choi, H., T.-K. Hong, X. He, and C.-E. Baag (2012). Seismic evidence for reverse activation of a paleo-rifting system in the East Sea (Sea of Japan), *Tectonophysics* **572/573,** 123–133.

Choi, S.-J., U. Chwae, H.-K. Lee, Y. Song, and I.-M. Kang (2012). Review on the Chugaryeong Fault, *J. Korean Soc. Econ. Envirom. Geol.* **45,** no. 4, 441–446 (in Korean with English abstract).

Chough, S. K., S.-T. Kwon, J.-H. Ree, and D.-K. Choi (2000). Tectonic and sedimentary evolution of the Korean Peninsula: A review and new view, *Earth Sci. Rev.* **52,** 175–235.

Chung, D., Y. Song, C. Park, I.-M. Kang, S.-J. Choi, and C. Khulganakhuu (2014). Reactivated timings of some major faults in the Chugaryeong Fault Zone since the Cretaceous Period, *J. Korean Soc. Econ. Envirom. Geol.* **47,** no. 1, 29–38 (in Korean with English abstract).

Crone, A. J., P. M. De Martini, M. N. Machette, K. Okumura, and J. R. Prescott (2003). Paleoseismicity of two historically quiescent faults in Australia: implications for fault behavior in stable continental regions, *Bull. Seismol. Soc. Am.* **93,** 1913–1934.

Degasperi, C., D. Slejko, A. Rebez, and M. Cergol (1991). Earthquakes felt in Trieste from the middle ages to the 18th century, *Tectonophysics* **193,** 53–63.

Frankel, A. (1995). Mapping seismic hazard in the central and eastern United States, *Seismol. Res. Lett.* **66,** 8–21.

Grünthal, G. (1998). *European Macroseismic Scale 1998*, Vol. 15, Cahiers Centre Européen de Géodynamique et de Séismologie, Luxembourg, 101 pp.

He, X., and T.-K. Hong (2010). Evidence for strong ground motion by waves refracted from the Conrad discontinuity, *Bull. Seismol. Soc. Am.* **100,** no. 3, 1370–1374.

Holbrook, J., W. J. Autin, T. M. Rittenour, S. Marshak, and R. J. Goble (2006). Stratigraphic evidence for millennial-scale temporal clustering of earthquakes on a continental-interior fault: Holocene Mississippi River floodplain deposits, New Madrid seismic zone, USA, *Tectonophysics* **420,** 431–454.

Hong, T.-K., and H. Choi (2012). Seismological constraints on the collision belt between the North and South China blocks in the Yellow Sea, *Tectonophysics* **570/571,** 102–113.

Hong, T.-K., C.-E. Baag, H. Choi, and D.-H. Sheen (2008). Regional seismic observations of the 9 October 2006 underground nuclear explosion in North Korea and the influence of crustal structure on regional phases, *J. Geophys. Res.* **113,** B03305, doi: 10.1029/2007JB004950.

Hong, T.-K., J. Lee, W. Kim, I.-K. Hahm, N. C. Woo, and S. Park (2017). The 12 September 2016 M_L 5.8 mid-crustal earthquake in the Korean Peninsula and its seismic implications, *Geophys. Res. Lett.* **44,** 3131–3138, doi: 10.1002/2017GL072899.

Hong, T.-K., J. Lee, S. Park, and W. Kim (2018). Time-advanced occurrence of moderate-size earthquakes in a stable intraplate region after a megathrust earthquake and their seismic properties, *Sci. Rep.* **8,** 13,331, doi: 10.1038/s41598-018-31600-5.

Hong, T.-K., S. Park, and S. E. Houng (2016). Seismotectonic properties and zonation of the far-eastern Eurasian plate around the Korean Peninsula, *Pure Appl. Geophys.* **173,** no. 4, 1175–1195.

Houng, S. E., and T.-K. Hong (2013). Probabilistic analysis of the Korean historical earthquake records, *Bull. Seismol. Soc. Am.* **103,** 2782–2796.

Katsumata, A. (1996). Comparison of magnitudes estimated by the Japan Meteorological Agency with moment magnitudes for intermediate and deep earthquakes, *Bull. Seismol. Soc. Am.* **86,** 832–842.

Kim, O. J. (1973). The straigraphy and geologic structure of the metamorphic complex in the Northwestern Area of the Kyonggi Massif, *J. Korean Soc. Econ. Envirom. Geol.* **6,** 201–218 (in Korean with English abstract).

Korea Meteorological Administration (2012). *Historical Earthquake Records in Korea (2~1904)*, Korea Meteorological Administration, Seoul, South Korea, 279 (in Korean).

Kossobokov, V. G., V. I. Keilis-Borok, D. L. Turcotte, and B. D. Malamud (2000). Implications of a statistical physics approach for earthquake hazard assessment and forecasting, *Pure Appl. Geophys.* **157,** 2323–2349.

Lee, J., T.-K. Hong, and C. Chang (2017). Crustal stress field perturbations in the continental margin around the Korean Peninsula and Japanese islands, *Tectonophysics* **718,** 140–149.

Lee, K., and W.-S. Yang (2006). Historical seismicity of Korea, *Bull. Seismol. Soc. Am.* **96,** 846–855.

Levret, A., J. C. Backe, and M. Cushing (1994). Atlas of macroseismic maps for French earthquakes with their principal characteristics, *Nat. Hazards* **10,** 19–46.

Li, Q., M. Liu, and S. Stein (2009). Spatiotemporal complexity of continental intraplate seismicity: Insights from geodynamic modeling and implications for seismic hazard estimation, *Bull. Seismol. Soc. Am.* **99,** 52–60.

Marsan, D., and O. Lenglinè (2008). Extending earthquakes' reach through cascading, *Science* **319,** 1076–1079.

McGuire, R. K. (1995). Probabilistic seismic hazard analysis and design earthquakes: closing the loop, *Bull. Seismol. Soc. Am.* **85,** 1275–1284.

Ministry of Construction and Transportation (1997). Investigation of seismic design standards (II): Seismic design standards and economic efficiency, Ministry of Construction and Transportation, *Report GOVP1199803210*, 493 pp., available at http://dl.nanet.go.kr/SearchDetailView.do?cn=MONO1199803210 (last accessed May 2020) (in Korean).

Miyazawa, M., and J. Mori (2009). Test of seismic hazardmap from 500 years of recorded intensity data in Japan, *Bull. Seismol. Soc. Am.* **99,** 3140–3149.

Musson, R. M. (1998). Intensity assignments from historical earthquake data: Issues of certainty and quality, *Ann. Geophys.* **41,** 79–91.

Musson, R. M., and I. Cecić (2012). Intensity and intensity scales, in *New Manual of Seismological Observatory Practice 2 (NMSOP-2)*, P. Bormann (Editor), Deutsches GeoForschungsZetrum (GFZ), Potsdam, Germany, 1–41.

Musson, R. M., G. Grünthal, and M. Stucchi (2010). The comparison of macroseismic intensity scales, *J. Seismol.* **14,** 413–428.

Oth, A., D. Bindi, S. Parolai, and D. Di Giacomo (2010). Earthquake scaling characteristics and the scale-(in)dependence of seismic energy-to-moment ratio: Insights from KiK-net data in Japan, *Geophys. Res. Lett.* **37,** L19304, doi: 10.1029/2010GL044572.

Park, S., and T.-K. Hong (2016). Joint determination of event epicenter and magnitude from seismic intensities, *Bull. Seismol. Soc. Am.* **106,** 499–511.

Park, S., and T.-K. Hong (2017). Regional seismic intensity anomalies in the Korean Peninsula and its implications for seismic-hazard potentials, *Pure Appl. Geophys.* **174,** no. 7, 2561–2579.

Pearthree, P. A., and S. S. Calvo (1987). The Santa Rita fault zone: Evidence for large magnitude earthquakes with very long recurrence intervals, Basin and Range province of southeastern Arizona, *Bull. Seismol. Soc. Am.* **77,** 97–116.

Richter, C. F. (1958). *Elementary Seismology*, W. H. Freeman, San Francisco, California.

Schwartz, D. P., and K. J. Coppersmith (1984). Fault behavior and characteristic earthquakes: Examples from the Wasatch and San Andreas fault zones, *J. Geophys. Res.* **89,** 5681–5698.

Scordilis, E. M. (2006). Empirical global relations converting M_S and m_b to moment magnitude, *J. Seismol.* **10,** 225–236.

Shimazaki, K., and T. Nakata (1980). Time-predictable recurrence model for large earthquakes, *Geophys. Res. Lett.* **7,** 279–282.

Sibol, M. S., G. A. Bollinger, and J. B. Birch (1987). Estimation of magnitudes in central and eastern North America using intensity and felt area, *Bull. Seismol. Soc. Am.* **77,** 1635–1654.

Stein, S. and S. Mazzotti (Editors) (2007). *Continental Intraplate Earthquakes: Science, Hazard, and Policy Issues*, Special Paper 425, Geological Society of America, Boulder, Colorado.

Stirling, M. W., S. G. Wesnousky, and K. R. Berryman (1998). Probabilistic seismic hazard analysis of New Zealand, *New Zeal. J. Geol. Geophys.* **41,** 355–375.

Termini, D., A. Teramo, and G. Arrigo (2005). A magnitude-felt area relation in the evaluation of the magnitude of historical earthquakes, *Pure Appl. Geophys.* **162,** 729–737.

Wang, J. (2004). Historical earthquake investigation and research in China, *Ann. Geophys.* **47,** 831–838.

Wood, H. O., and F. Neumann (1931). Modified Mercalli intensity scale of 1931, *Bull. Seismol. Soc. Am.* **21,** 277–283.

Manuscript received 6 January 2020
Published online 14 July 2020